

# Multichannel quantum defect theory: a quantum Poincaré map.

F. Leyvraz<sup>a,b</sup>, R. A. Méndez-Sánchez<sup>b,1</sup>,  
M. Lombardi<sup>c,2</sup> and T. H. Seligman<sup>a,b</sup>

<sup>a</sup>*Centro de Ciencias Físicas University of Mexico (UNAM), Cuernavaca, Mexico*

<sup>b</sup>*Centro Internacional de Ciencias, Cuernavaca, Mexico*

<sup>c</sup>*Laboratoire de Spectrométrie Physique, CNRS and Université  
Joseph-Fourier-Grenoble (UMR 5588), BP87,  
F-38402 Saint-Martin-d'Hères Cédex, France*

---

## Abstract

The multichannel quantum defect theory (MQDT) can be reinterpreted as a quantum Poincaré map in representation of angular momentum. This has two important implications: we have a paradigm of a true quantum Poincaré map without semi-classical input and we get an entirely new insight into the significance of MQDT.

PACS: 05.45.Mt; 33.80.Rv; 03.65.Sq

---

In recent years there has been a rapidly growing interest in the quantum Poincaré map (QPM) [1–10], i.e. the quantization of a classical Poincaré map, for a time independent Hamiltonian system. Bogomolny[1] started out with a semi-classical formulation. Among other things he shows that unitarity of the representation is reached in the limit  $\hbar \rightarrow 0$ , while this is only approximate for finite  $\hbar$  [8]. Prosen [4] gives an elegant general solution to the unitarity problem at the expense of obtaining an infinite matrix for the QPM. The semi-classical approach common to most discussions causes a number of problems that make the use of this new and powerful tool a little obscure. With other words, the quantum Poincaré section implicitly defined by Bogomolny, lacks a paradigmatic example where a quantum treatment can be performed properly throughout and leads to a finite unitary matrix.

Multichannel quantum defect theory (MQDT) [11–15] and its classical limit [16–18] will be shown to provide the framework for such a paradigm. Indeed

---

<sup>1</sup> Present address: Fachbereich 7, Physik, Universität G. H. Essen, 45117 Essen

<sup>2</sup> Corresponding author; Fax: +33 476 514 544; e-mail: Maurice.Lombardi@ujf-grenoble.fr

we shall see that a simplified model of the Rydberg molecule allows to construct a classical Poincaré map on the unit sphere, whose exact quantization is provided by MQDT. Thus the result is necessarily entirely quantal, exactly unitary and for finite  $\hbar$  given in terms of a finite matrix. We shall show that the results commonly derived for MQDT are directly properties of the unitary representation of this classical map as obtained by MQDT.

After a short description of the model for a Rydberg molecule and the simplification introduced in Ref. [16], we proceed to give the quantum map for this case explicitly. We illustrate the two important aspects of our result by two applications. First the new interpretation allows modifications of the MQDT method, that prove particularly effective in near integrable systems. Second we proceed to show by way of examples that the properties of this map are relevant to the study of chaos and order in this system.

Simplifying to the most basic case, these molecules can be viewed as a rotating system with positive charge and cylindrical symmetry that binds one electron in an orbit that is at large distances hydrogenic. The classical limit of the MQDT is the following classical model [16]: The motion is composed of two consecutive steps. (i) when the electron is far from the molecular core (i.e. most of the time for a Rydberg electron) it feels only the Coulomb part ( $-1/r$ ) of the potential. Its orbit is hydrogenic and its angular momentum  $\mathbf{L}$  is fixed in the laboratory reference frame. Meanwhile the core rotates freely with an angular momentum  $\mathbf{N}$  which is also fixed in the laboratory frame. The total angular momentum  $\mathbf{J} = \mathbf{L} + \mathbf{N}$  is always conserved. In the molecular reference frame, the  $OZ$  axis is the cylindrical symmetry axis of the core. The core angular momentum  $\mathbf{N}$  points in a perpendicular direction, taken as the  $OX$  axis. The angles  $\theta_e$  and  $\phi_e$  are the polar and azimuthal angles respectively of the electronic angular momentum  $\mathbf{L}$  in this frame. During this step,  $\mathbf{L}$  rotates freely around the  $OX$  axis. (ii) during the so called "collision" step, the electron senses also the cylindrically symmetric short range part of the potential of the core. Aside from the energy and  $\mathbf{J}$ , the projection of  $\mathbf{L}$  onto the core axis  $\Lambda = L \cos \theta_e$  is conserved due to the cylindrical symmetry of the core. We will add an extra, simplifying, hypothesis, namely that the magnitude  $L$  of  $\mathbf{L}$  remains constant[16]. This is justified for Rydberg Molecules at least for small  $L$ 's, but the classical and quantum map with this approximation exist for all  $L$ . Thus the collision can be described by a  $\theta_e$ -dependent rotation of  $\mathbf{L}$  around the core axis. The simplest form of this rotation compatible with the symmetry is [16]:  $\delta\phi_e = K \cos \theta_e$ , where  $K$  is a coupling constant. This simplification is not essential. Notice further that the conservation of the total angular momentum  $\mathbf{J}$  implies that the molecular core feels a simultaneous recoil which changes the direction and magnitude of  $\mathbf{N}$ . This change of  $N$  in turn entails a change of the rotational energy  $E_N$  of the core and because of conservation of total energy a change of the energy  $E_e$  of the electron. This exchange of energy makes this model much richer than the kicked spin model [19] (which

is its limit when  $L \ll J$ , where this recoil can be neglected). In particular the energy of the electron may become positive after the collision, allowing to treat on equal footing bound and unbound (ionized) states. Possibility of chaotic motion comes from the conflict of these two steps, which consist of two rotations around distinct axes with different laws. The classically chaotic case can be obtained by increasing the coupling  $K$ . Near-integrable cases can be obtained for small coupling or at resonance, i.e. when the period of the electron is a multiple of half the period of rotation of the core.

The quantum problem is solved by using the MQDT. The configuration space is divided by a sphere of radius  $r_0$  in a collision ( $r < r_0$ ) and an asymptotic region ( $r > r_0$ ) for the motion of the electron.  $r_0$  is of the order of the core size and is chosen such that in the asymptotic region the potential acting on the electron is only Coulombic, whereas in the collision region it feels both Coulomb and cylindrical potential. The wave functions for both regions are joined appropriately at  $r = r_0$ . The conflict between the two motions is expressed in quantum mechanics by the existence for the wave function of two bases with different good quantum numbers (in addition to  $J, J_z, L$  and total energy  $E$ ). At short distance the Born Oppenheimer basis is appropriate. The Rydberg electron is strongly bound to the core, thus quantized in the molecular reference frame and the additional good quantum number is  $\Lambda$ . At long distances the collision basis is appropriate. Here the electron is uncoupled from the core and the angular momentum  $N$  of the core remains a good quantum number. The collision is described by phase shifts  $\mu_\Lambda$ , which are identical to collision phase shifts if the total energy is positive enough for all channels to be open, and which are related to the classical  $K$  parameter by  $\mu_\Lambda = \mu_0 - (K/4\pi L)\Lambda^2$ .

We focus on the completely bound situation, when total energy is low enough for the electron energy to be always negative whatever the value of  $N$  within the allowed range  $[J - L, J + L]$ . Demanding that the electron wave function goes to zero when  $r \rightarrow \infty$  leads to demanding that the following determinant vanishes [15], *i.e.*

$$\det \mathbf{S} = \det \{U_{N\Lambda} \sin(\pi(\mu_\Lambda + \nu_N))\} = 0, \quad (1)$$

where the *unitary*  $U$  matrix given by

$$U_{N,\Lambda} = \langle L, -\Lambda, J, \Lambda | N, 0 \rangle (-1)^{J-N+\Lambda} (2 - \delta_\Lambda, 0)^{1/2}. \quad (2)$$

relates the two conflicting bases through a Clebsh Gordan coefficient. The principal (non integer) action  $\nu_N(E)$  of the Coulomb electron, is related to the electron energy through  $E = E_N + E_e = N(N+1)/(2I) - 1/(2\nu_N^2)$ , where  $I$  is the moment of inertia of the core, and we use atomic units ( $e = m = \hbar = 1$ ).

Corresponding wave functions are the eigenkets of  $\mathbf{S}$  for the eigenvalue zero, labeled by  $\Lambda$  in the Born Oppenheimer basis:

$$\mathbf{S}|A_\Lambda\rangle = 0. \quad (3)$$

Similarly the eigenbras  $\langle B_N|$  of  $\mathbf{S}$  (eigenkets of  $\mathbf{S}^t$ ), labeled by  $N$  describe the corresponding wave function in the collision basis.

To proceed notice first that  $\mathbf{S}$  is the imaginary part of a complex *unitary* matrix

$$\mathbf{E} = \mathbf{C} + i\mathbf{S} = \{U_{N\Lambda} \exp(i\pi(\mu_\Lambda + \nu_N))\}. \quad (4)$$

This non symmetrical matrix maps the  $N$  basis on the  $\Lambda$  basis: it is *half* the QPM we look for, and describes the motion between apogee and perigee. From it we can construct two QPM, which, by construction, turn out to be *symmetrical unitary* complex matrices.

$\mathbf{E}^t\mathbf{E}$  operates in Born Oppenheimer  $\Lambda$  space, and is the exact quantization of a classical Poincaré map. The latter is nearly the classical map used in refs. [16,17]. That map on the unit sphere described the position of  $\mathbf{L}$  in the molecular frame immediately after the collision, whereas the present map describes the position of  $\mathbf{L}$  in the middle of the collision (perigee). That this matrix is the  $T$  matrix defined by Bogomolny[1] to quantize a Poincaré map will be shown by proving that the eigenvalues and eigenfunctions of the entire system result from

$$\det(1 - T(E_n)) = 0, \quad (5)$$

i.e. Bogomolny's equation for the quantized energy  $E_n$ . Indeed at quantized energies given by Eq. (1)

$$\mathbf{E}^t\mathbf{E}|A_\Lambda\rangle = 1|A_\Lambda\rangle, \quad (6)$$

which implies (5). To prove this key point first notice that unitarity of  $\mathbf{E}$ , namely  $\mathbf{E}^\dagger\mathbf{E} = (\mathbf{C}^t - i\mathbf{S}^t)(\mathbf{C} + i\mathbf{S}) = \mathbb{I}$ , leads to  $\mathbf{C}^t\mathbf{C} + \mathbf{S}^t\mathbf{S} = \mathbb{I}$  and  $\mathbf{C}^t\mathbf{S} = \mathbf{S}^t\mathbf{C}$ . Then  $\mathbf{E}^t\mathbf{E} = (\mathbf{C}^t + i\mathbf{S}^t)(\mathbf{C} + i\mathbf{S}) = \mathbb{I} - 2\mathbf{S}^t\mathbf{S} + 2i\mathbf{C}^t\mathbf{S}$ , so that if  $\mathbf{S}|A_\Lambda\rangle = 0$  then  $\mathbf{E}^t\mathbf{E}|A_\Lambda\rangle = \mathbb{I}|A_\Lambda\rangle$ .

Conversely  $\mathbf{E}\mathbf{E}^t$  operates in collision  $N$  space and corresponds to a classical map between apogee and apogee in the laboratory frame.

We will now compare the traditional way of solving MQDT to the one implied by our QPM. The traditional way is to look for zeros of the determinant of the

non-symmetric matrix  $\mathbf{S}$  of Eq. (1), all of whose elements depend in a complex way on energy through  $\nu_N(E)$ . It is computed by a LU or a SVD method followed by a root searching algorithm [21,16]. The present method is to look for eigenphases of  $\mathbf{E}^t\mathbf{E}$  or  $\mathbf{E}\mathbf{E}^t$ . They are computed by the diagonalization of a symmetrical unitary matrix. This is efficient and unproblematic because it diagonalizes in an orthonormal basis. Finally we search the zeros of the resulting eigenphases.

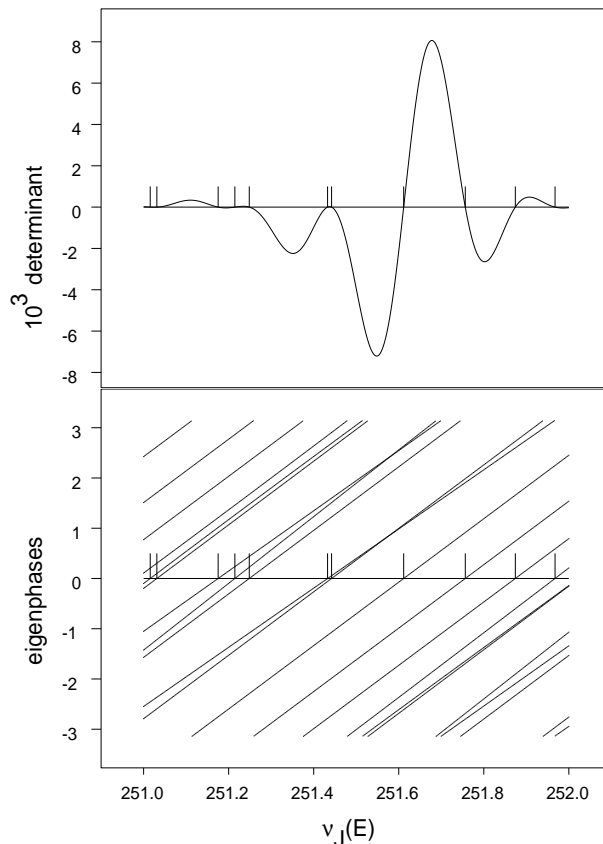


Fig. 1. Comparison of Determinant and Eigenphases methods to solve the MQDT problem. Abscissa axis is energy on a scale  $\nu_N(E)$  for the middle  $N = J$  value.

The situation is sketched in Fig. 1. The search for zeros of eigenphases which vary nearly linearly with energy is obviously much simpler than the search of zeros of a determinant which is sometimes nearly tangent to the horizontal axis. Moreover, in this case of near tangency we had problems to converge the wave functions because the eigenfunction switches between two nearly orthogonal values in a very narrow energy range [17], requiring the use of the more efficient but slower SVD algorithm. Such a situation occurs frequently in nearly integrable cases, due to the lack of level repulsion. The diagonalization, on the contrary, gives always correctly the orthogonal eigenfunctions even if eigenvalues are very close.

The implications of this procedure for the study of quantum chaos is of great

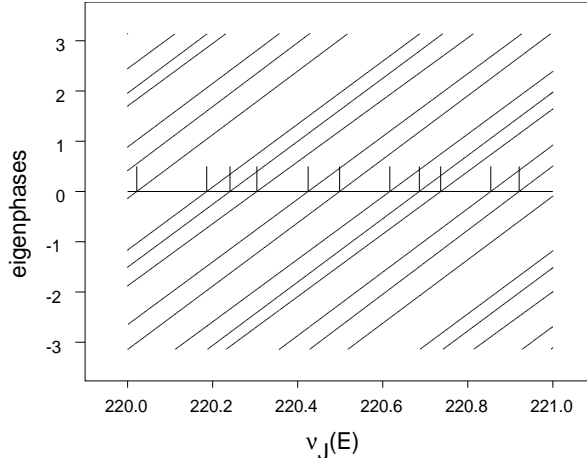


Fig. 2. Eigenphases in a chaotic case.

interest. Figure 2 displays a chaotic situation. Comparing eigenphases in the near integrable (Fig. 1) and chaotic (Fig. 2) situations, we see that in the first case the phases as a function of energy display avoided crossings of straight lines running at different angles while for the second case these lines are practically parallel. This shows that the drift of eigenphases as a function of energy displays presence or absence of level repulsion or spectral rigidity more obviously than the energy levels themselves. This consideration is important in relation with the theory put forward by two of us [22], which relates Random Matrix Properties of eigenvalues of a quantum system to properties of invariance under canonical transformations of the structure of the corresponding classical system (structural invariance). This theory was developed for maps such as the scattering map, the stroboscopic map or the Poincaré map leading to results about their unitary representations, i.e. about eigenphases. To transfer statistical properties of eigenphases of the QPM to energy eigenvalues, it is necessary that the drift of eigenphases as a function of energy be nearly parallel for all phases. Analytic evidence that this must be true for chaotic systems is given in [22,23], in agreement with the numerical results shown in Fig. 2. To put this on a more quantitative basis we display on Fig. 3 histograms of the distributions of the velocities of the eigenphases curves. The chaotic case has a narrow distribution while the integrable one shows long tails. The present study is much more convincing in that respect than another one for billiards using directly Bogomolny theory[23], which is garbled by the non unitarity of the  $T$  matrix for finite  $\hbar$ .

The difference seen in Fig. 3 for the near integrable and the chaotic case is remarkable and it is thus tempting to consider the eigenphase velocity distribution as another signature of classical chaos in quantum mechanics. While the narrow distribution for chaotic systems is typical, the tails for the integrable systems are not generic: they depend on the details of the partition of phase space by separatrices. In other examples [23] tails have different shapes.

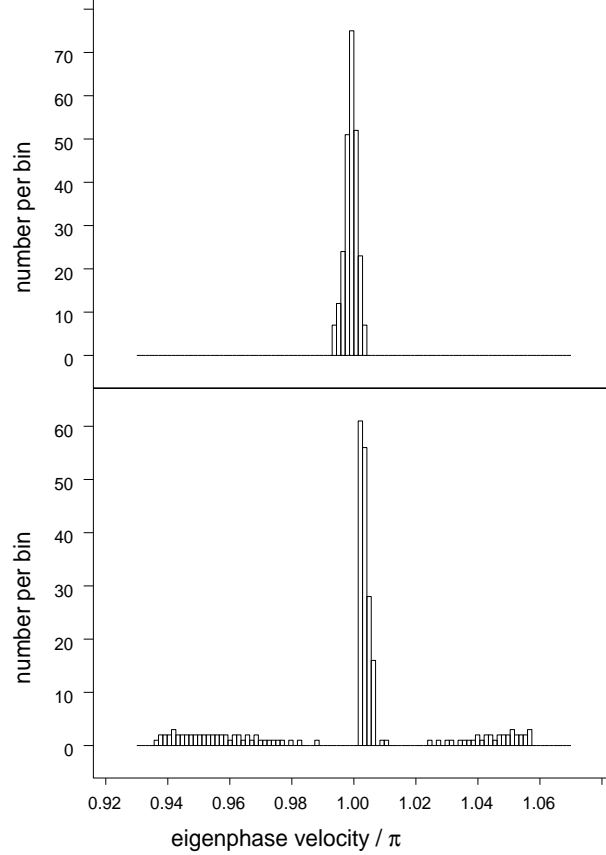


Fig. 3. Histograms of the velocities of the eigenphases curves for a given energy. Top: chaotic case, bottom: integrable case. These histograms correspond to the same classical parameters as in Figs. 1 and 2, but  $\hbar$  has been divided by 25 to increase statistics

Summarizing: in this paper we proposed to interpret the multichannel quantum defect theory as a quantum Poincaré map. This was implemented in detail in the approximation that the absolute value of the electron angular momentum is conserved, but it is quite clear that it is true in general. The new interpretation allows for a more stable and efficient way to find solutions to MQDT, particularly for near-degenerate levels. Beyond that, the approximate system has been used to exemplify quantum features of classically chaotic systems. This can be now extended to use MQDT as a paradigm for QPM. Indeed a study of the velocity distribution of eigenphases confirms properties expected from other studies.

This work was partially supported by DGAPA (UNAM) project IN... and the CONACYT grant 25192-E

## References

- [1] E. B. Bogomolny, Nonlinearity 5 (1992) 805; Chaos 2 (1992) 5; Comments At. Mol. Phys. 25 (1990) 67.
- [2] E. Doron and U. Smilansky, Nonlinearity 5 (1992) 1055.
- [3] B. Dietz and U. Smilansky, Chaos 3 (1993) 581.
- [4] T. Prosen, Physica D 91 (1996) 244.
- [5] T. Szeredi, J. H. Lefebvre, and D. A. Goodings, Phys. Rev. Lett. 71 (1993) 2891; Nonlinearity 7 (1994) 1463.
- [6] M. C. Gutzwiller, Chaos 3 (1993) 591.
- [7] D. A. Goodings and N. D. Whelan, J. Phys. A 31 (1998) 7521.
- [8] M. R. Haggerty, Phys. Rev. E 52 (1995) 389.
- [9] B. Georgeot and R. E. Prange, Phys. Rev. Lett. 74 (1995) 2851.
- [10] R. E. Prange, Phys. Rev. Lett. 77 (1996) 2447.
- [11] M. Seaton, Rep. Progr. Phys. 46 (1983) 167.
- [12] U. Fano, Phys. Rev. A 2 (1970) 353.
- [13] U. Fano and A. R. P. Rau, Atomic Collisions and Spectra (Academic Press, Orlando, 1986).
- [14] C. Greene, U. Fano, and G. Srinati, Phys. Rev. A 19 (1979) 1485.
- [15] M. C. Bordas, M. Broyer, J. Chevalerey, P. Labastie, and S. Martin, J. Phys. (Paris) 46 (1985) 27.
- [16] M. Lombardi, P. Labastie, M. Bordas, and M. Broyer, J. Chem. Phys. 89 (1988) 3479.
- [17] M. Lombardi and T. Seligman, Phys. Rev. A 47 (1993) 3571.
- [18] B. Dietz, M. Lombardi, and T. H. Seligman, Phys. Lett. A 215 (1996) 181.
- [19] K. Nakamura, Y. Okasaki, and A. R. Bishop, Phys. Rev. Lett. 57 (1986) 5.
- [20] K. Husimi, Proc. Phys. Soc. Japan 22 (1940) 264.
- [21] W. H. Press, B. P. Flannery, S. A. Teukolsky, and W. T. Vetterling, Numerical Recipes (Cambridge University Press, New York, 1988).
- [22] F. Leyvraz and T. H. Seligman, Phys. Lett. A 168 (1992) 348; in Proceedings IV Wigner Symposium (World Scientific, Singapore, 1995); T. H. Seligman, Quantum Chaos (Cambridge University Press, New York, 1995).
- [23] F. Leyvraz, R. A. Mendez, and T. H. Seligman, chao-dyn/9902009; R. A. Méndez-Sánchez, Ph.D. thesis, UNAM, Mexico, 1999.